Meccanica (2014) 49:2551–2569
DOI 10.1007/s11012-014-0044-5

Nonlocal elasticity: an approach based on fractional calculus

Alberto Carpinteri · Pietro Cornetti · Alberto Sapora

Received: 8 January 2014 / Accepted: 13 August 2014 / Published online: 25 September 2014

Abstract Fractional calculus is the mathematical subject dealing with integrals and derivatives of non-integer order. Although its age approaches that of classical calculus, its applications in mechanics are relatively recent and mainly related to fractional damping. Investigations using fractional spatial derivatives are even newer. In the present paper spatial fractional calculus is exploited to investigate a material whose nonlocal stress is defined as the fractional integral of the strain field. The developed fractional nonlocal elastic model is compared with standard integral nonlocal elasticity, which dates back to Eringen's works. Analogies and differences are highlighted. The long tails of the power law kernel of fractional integrals make the mechanical behaviour of fractional nonlocal elastic materials peculiar. Peculiar are also the power law size effects yielded by the anomalous physical dimension of fractional operators. Furthermore we prove that the fractional nonlocal elastic medium can be seen as the continuum limit of a lattice model whose points are connected by three levels of springs with stiffness decaying with the power law of the distance between the connected points. Interestingly, interactions between bulk and surface material points are taken distinctly into account by the fractional model. Finally, the fractional differential equation in terms of the displacement function along with the proper static and kinematic boundary conditions are derived and solved implementing a suitable numerical algorithm. Applications to some example problems conclude the paper.

Keywords Nonlocal elasticity · Fractional calculus · Size effects

1 Introduction

Fractional calculus is the branch of mathematics dealing with integrals and derivatives of arbitrary order. The elegance and the conciseness of fractional operators in describing smoothly the transition between distinct differential equations, and hence between different models, are attracting an increasing numbers of scientists and researchers in many fields, like economics, mathematical physics or engineering.

For what concerns mechanics, a well-established field of application of fractional calculus is viscoelasticity (for a review see [1]. In such a case, the fractional derivatives are performed with respect to the time variable and the nonlocal nature of fractional derivative is exploited to take the long-tail memory of the strain history into account. A recent paper illustrating the state-of-the-art about dynamic problems for fractionally damped structure is the one by Rossikhin and Shitikova [2].

A. Carpinteri · P. Cornetti (✉) · A. Sapora
Department of Structural, Building and Geotechnical Engineering, Politecnico di Torino, Corso Duca degli Abruzzi 24, 10129 Turin, Italy
e-mail: pietro.cornetti@polito.it

Mechanical applications of spatial fractional derivatives are more recent. They have been considered firstly within the study of anomalous diffusion processes (to cite but a few, see [3–7]) and later within the framework of solid mechanics, following two directions. The former direction of research aims to explore the connection between fractional calculus and fractal geometry, i.e. the study of sets with non-integer dimensions and self-similar scaling properties. Without claiming to be exhaustive, here we can cite: the paper by Carpinteri and Cornetti [8], where fractality is the consequence of fractal patterns arising in deformation and damage of disordered materials; the works by Carpinteri et al. [9] and by Tarasov [10] where a fractal mass density related to a self-similar pore structures is considered; and the paper by Michelitsch et al. [11], where fractal geometry comes from the assumption of self-similar elastic properties. The strength of such an approach are the non-integer physical dimensions provided by both fractal geometry and fractional operators.

The latter research direction exploits the fractional calculus formalism to describe the mechanics of nonlocal materials characterized by long-range interactions decaying with the power law of the distance [12]. The first attempt to relate fractional calculus and nonlocal continuum mechanics is probably due to Lazopoulos [13], while Di Paola and Zingales [14] developed a point-spring model with nonlocal interactions whose equilibrium equation can be partly described by means of fractional derivatives. Later, Carpinteri et al. [15, 16] considered a material whose constitutive law is of fractional type, highlighting its connection with Eringen nonlocal elasticity. Interestingly, the same basic equations were derived by Atanackovic and Stankovic [17] starting from a different point of view, i.e. considering a fractional nonlocal strain measure.

The previous results have been then extended to dynamic analysis and wave propagation in fractional nonlocal elastic media [18–20]. Other fractional approaches to nonlocal elasticity are the ones by Drapaca & Sivaloganathan [21] and Tarasov [22]. Particularly, the last model sounds promising: fractional nonlocal elastic media are interpreted as the continuum limit of discrete systems with long-range interactions and the transition between strong (integral) and weak (gradient) nonlocal elasticity in terms of fractional operators emerges rather naturally [23].

Aim of the present paper is to give a deeper insight to the preliminary analysis provided in [16]. After a brief introduction, in Sect. 2 the basic definitions and properties of fractional calculus are given; an original expression of the Riesz fractional derivative of order between 1 and 2, useful for the subsequent analysis, is proved. In Sect. 3, the fractional constitutive equation characterizing fractional nonlocal elastic media is proposed, analyzed and compared with the one valid for Eringen nonlocal elasticity. Similarities and differences are highlighted. In Sect. 4, the one-dimensional model of a fractional nonlocal elastic bar is investigated. The fractional differential equation governing the mathematical problem is provided along with its proper static and kinematic boundary conditions. Equivalence with a discrete lattice model is given on the basis of the results of Sect. 2. Section 5 deals with numerical simulations: a suitable algorithm to solve numerically the fractional differential problem is set and applied to some example problems. Section 6 is voted to conclusions.

2 Fractional calculus and fractional operators

In the present section we will provide a short overview of fractional calculus, focussing our attention to the formulae that will be exploited in the following sections. The interested reader is referred to the books and treatises dealing with this peculiar branch of mathematics, such as [24–26].

The birth of fractional calculus is conventionally set to 1695, when the father of the calculus, Leibniz, wrote a letter to de L'Hôpital about the possibility of defining a derivative of order 1/2 of a function. Although, as we shall see, the theory developed later generalizes the order of derivation to any real (or even complex) order, this is the reason why this branch of the calculus is still named as fractional.

Fractional integral can be introduced in a number of different ways. The most common is the generalization to non-integer values of Cauchy formula for repeated integrations. Hence we define the fractional integral of order β ($\beta \in \Re^{+}$) as:

$$I_{a+}^{\beta} f(x) = \frac{1}{\Gamma(\beta)} \int_{a}^{x} \frac{f(t)}{(x-t)^{1-\beta}} \, dt \tag{1}$$

where Γ is the Gamma function and a is the so-called lower bound. For $\beta = 0$ the fractional integral reverts to the function $f(x)$ itself, whereas for positive integer values it coincides with the n-th primitive of $f(x)$ vanishing at $x = a$. The Riemann–Liouville fractional derivative of order β is defined as the (integer) derivative of order n ($n \in N^+$) of the fractional integral of order ($n - \beta$), where n is the smallest integer larger than β:

$$D^{\beta}_{a+}f(x) = D^n[I^{n-\beta}_{a+}f(x)] \tag{2}$$

For the relevant case $0 < \beta < 1$, Eq. (2) reads:

$$D^{\beta}_{a+}f(x) = D[I^{1-\beta}_{a+}f(x)] = \frac{1}{\Gamma(1-\beta)}\frac{\mathrm{d}}{\mathrm{d}x}\int_a^x \frac{f(t)}{(x-t)^{\beta}}\mathrm{d}t \tag{3}$$

From Eq. (3) we immediately see that the fractional derivative is a nonlocal operator, although nonlocality vanishes for β tending to 0 or 1, when the fractional derivative equals the function itself and its first derivative, respectively.

Equations (1)–(3) represent the so-called left (or forward) fractional operators. Analogously, introducing the so-called upper bound b, it is possible to define the right (or backward) integrals and derivatives respectively as:

$$I^{\beta}_{b-}f(x) = \frac{1}{\Gamma(\beta)}\int_x^b \frac{f(t)}{(t-x)^{1-\beta}}\mathrm{d}t \tag{4}$$

and:

$$D^{\beta}_{b-}f(x) = (-D)^n[I^{n-\beta}_{b-}f(x)] \underset{n=1}{=} -\frac{1}{\Gamma(1-\beta)}\frac{\mathrm{d}}{\mathrm{d}x}\int_x^b \frac{f(t)}{(t-x)^{\beta}}\mathrm{d}t \tag{5}$$

Among the few simple, yet powerful, results of fractional calculus is the β-derivative of the power function $(x - a)^{\gamma}$. It reads:

$$D^{\beta}_{a+}(x-a)^{\gamma} = \frac{\Gamma(\gamma+1)}{\Gamma(\gamma-\beta+1)}(x-a)^{\gamma-\beta} \tag{6}$$

Analogously:

$$D^{\beta}_{b-}(b-x)^{\gamma} = \frac{\Gamma(\gamma+1)}{\Gamma(\gamma-\beta+1)}(b-x)^{\gamma-\beta} \tag{7}$$

Note that Eqs. (6–7) hold true also for negative β values, when they provide the expression of the fractional integral of order (−β). Moreover, from Eqs. (6–7) it is evident that the fractional derivative of the unity (corresponding to $\gamma = 0$) is not null unless the order of derivation β is a positive integer.

Equation (2) however is not the only way to generalize standard derivatives to non-integer orders. For instance, another possibility is to define the fractional derivative of order β as the fractional integral of order ($n - \beta$) of the (integer) derivative of order n. In this way we obtain the so-called Caputo definition of the (left) fractional derivative:

$${}_{C}D^{\beta}_{a+}f(x) = I^{n-\beta}[D^n_{a+}f(x)] \tag{8}$$

For $0 < \beta < 1$, it reads:

$${}_{C}D^{\beta}_{a+}f(x) = I^{1-\beta}_{a+}[D\,f(x)] = \frac{1}{\Gamma(1-\beta)}\int_a^x \frac{f'(t)}{(x-t)^{\beta}}\mathrm{d}t \tag{9}$$

Its right counterpart is:

$${}_{C}D^{\beta}_{b-}f(x) = I^{n-\beta}_{b-}[(-D)^n f(x)] \underset{n=1}{=} -\frac{1}{\Gamma(1-\beta)}\int_x^b \frac{f'(t)}{(t-x)^{\beta}}\mathrm{d}t \tag{10}$$

While the Riemann–Liouville fractional derivative of a constant is not zero, Eq. (8) shows that the corresponding Caputo derivative vanishes, as it happens for integer order derivative. Thus, Caputo fractional derivative is usually more practical for applications. Another important observation is that, while the forward fractional derivatives coincide with their integer counterpart when β is a positive integer, the backward fractional derivatives (either Riemann–Liouville or Caputo) equals the corresponding even derivative when n is even and the *opposite* of its odd derivative when n is odd.

A general result in fractional analysis states that the Caputo fractional derivatives (either forward or backward) of a function $f(x)$ are equal to the Riemann–Liouville derivatives provided that the polynomial of order $n - 1$ (evaluated either in $x = a$ or $x = b$) is subtracted from the function itself:

$${}_{C}D^{\beta}_{a+}f(x) = D^{\beta}_{a+}\left[f(x) - \sum_{k=0}^{n-1}\frac{f^{(k)}(a)}{k!}(x-a)^k\right] \tag{11a}$$

$$ {}_{C}D^{\beta}_{b-}f(x) = D^{\beta}_{b-}\left[f(x) - \sum_{k=0}^{n-1}\frac{f^{(k)}(b)}{k!}(b-x)^{k}\right] \tag{11b} $$

For the particular case $0 < \beta < 1$, Eqs. (11) simplify into:

$$ {}_{C}D^{\beta}_{a+}f(x) = D^{\beta}_{a+}[f(x) - f(a)] \tag{12a} $$

$$ {}_{C}D^{\beta}_{b-}f(x) = D^{\beta}_{b-}[f(x) - f(b)] \tag{12b} $$

By means of Eqs. (6) and (7) it is possible to invert Eqs. (11):

$$ D^{\beta}_{a+}f(x) = {}_{C}D^{\beta}_{a+}f(x) + \sum_{k=0}^{n-1}\frac{f^{(k)}(a)}{\Gamma(1+k-\beta)}(x-a)^{k-\beta} \tag{13a} $$

$$ D^{\beta}_{b-}f(x) = {}_{C}D^{\beta}_{b-}f(x) + \sum_{k=0}^{n-1}(-1)^{k}\frac{f^{(k)}(b)}{\Gamma(1+k-\beta)}(b-x)^{k-\beta} \tag{13b} $$

A third widely used definition of fractional derivative is due to Marchaud [25]. It will be exploited to give a mechanical interpretation to the fractional nonlocal constitutive equation we shall introduce in the next section. Marchaud definitions of the left and right fractional derivatives read:

$$ D^{\beta}_{a+}f(x) = \frac{1}{\Gamma(1-\beta)}\left[\frac{f(x)}{(x-a)^{\beta}} + \beta\int_{a}^{x}\frac{f(x)-f(t)}{(x-t)^{1+\beta}}\,\mathrm{d}t\right] \tag{14a} $$

$$ D^{\beta}_{b-}f(x) = \frac{1}{\Gamma(1-\beta)}\left[\frac{f(x)}{(b-x)^{\beta}} + \beta\int_{x}^{b}\frac{f(x)-f(t)}{(t-x)^{1+\beta}}\,\mathrm{d}t\right] \tag{14b} $$

Differently from Caputo definitions (9) and (10), the first derivative $f'(t)$ in the integral is now replaced by the incremental ratio with respect to the value in x: $[f(x) - f(t)]/(x - t)$. It is easy to check that, under suitable regularity assumptions for the function $f(x)$, Eqs. (14) can be obtained by integrating by parts Eqs. (9–10). Although Eqs. (14) are usually given as definitions, we will use the same symbol for both Marchaud and Riemann–Liouville fractional derivatives since, for a wide class of functions, they coincide with Riemann–Liouville definitions (3) and (5). However it is important to emphasize that, while Riemann–Liouville and Caputo definitions of fractional derivative hold for any positive β values, Marchaud definitions hold only for orders of derivation lower than unity ($0 < \beta < 1$).

Finally, it is possible to introduce the Riesz fractional integrals and derivatives, defined as the sum of the forward and backward fractional operators up to a multiplicative factor:

$$ I^{\beta}_{a,b}f(x) = \frac{1}{2}\left[\,I^{\beta}_{a+}f(x) + I^{\beta}_{b-}f(x)\right] = \frac{1}{2\Gamma(\beta)}\int_{a}^{b}\frac{f(t)}{|x-t|^{1-\beta}}\,\mathrm{d}t \tag{15a} $$

$$ D^{\beta}_{a,b}f(x) = \frac{1}{2}\left[D^{\beta}_{a+}f(x) + D^{\beta}_{b-}f(x)\right] \tag{15b} $$

Note that the multiplicative constant, here taken simply equal to 1/2 following e.g. [27], can vary according to different fractional calculus treatises. Among the various properties of the Riesz operators, it is here important to observe that, while the fractional integral (1) spans from the integrand function $f(x)$ to its primitive (depending on x as well) as β increases from 0 to 1, the Riesz integral (15a) varies from the integrand function $f(x)$ to half of its definite integral on the interval $[a,b]$, which does not depend on x. For the same reason, the Riesz derivative (15b) vanishes when β is an odd integer, while it coincides with the corresponding integer derivative when β is even.

In Sect. 4 we will show that the fractional nonlocal elastic model can be seen as the continuum limit of a discrete lattice model. To this aim we need to express the Riesz derivative (15b) of order comprised between 0 and 2 in a Marchaud-like form (Eqs. 14). Since, at our best knowledge, this result is original, herein we provide the details of the proof. However, it is worth noting that a similar result for fractional operators defined on an infinite domain (the so-called Weyl fractional integrals), has been proved by Gorenflo & Mainardi [28] extending a previous result by Samko et al. [25]. For fractional operators defined on infinite domains see also [29, 30].

We start observing that, while for $0 < \beta < 1$ our task is immediately accomplished by summing up Eqs. (14a) and (14b), for $1 < \beta < 2$ (which is our main range of interest) the problem is not trivial since, as noted above, Marchaud definition of fractional derivative holds true only for order of derivation lower than unity: in fact, for $\beta > 1$, the integrals at the right hand side of Eqs. (14) diverge. However we can write the Marchaud (left) fractional derivative of order $0 < \alpha < 1$ of the first derivative, which, on the basis of Eq. (14a), reads:

$$D^{\alpha}_{a+}f'(x) = \frac{f'(x)}{\Gamma(1-\alpha)(x-a)^{\alpha}} + \frac{\alpha}{\Gamma(1-\alpha)}\int_a^x \frac{f'(x)-f'(t)}{(x-t)^{1+\alpha}}\,\mathrm{d}t \tag{16}$$

Then we split the integral at the right hand side and apply the integration by parts formula to the second addend:

$$\int_a^x \frac{f'(t)}{(x-t)^{1+\alpha}}\mathrm{d}t = \left[\frac{f(t)-f(x)}{(x-t)^{1+\alpha}}\right]_{t=a}^{t=x} - (1+\alpha)\int_a^x \frac{f(t)-f(x)}{(x-t)^{2+\alpha}}\mathrm{d}t \tag{17}$$

so that Eq. (16) becomes:

$$D^{\alpha}_{a+}f'(x) = \frac{1}{\Gamma(1-\alpha)}\left\{\frac{f'(x)}{(x-a)^{\alpha}} + \alpha f'(x)\int_a^x \frac{\mathrm{d}t}{(x-t)^{1+\alpha}} + \alpha\lim_{t\to x^-}\left[\frac{f(x)-f(t)}{(x-t)^{1+\alpha}}\right] - \alpha\frac{f(x)-f(a)}{(x-a)^{1+\alpha}} - \alpha(1+\alpha)\int_a^x \frac{f(x)-f(t)}{(x-t)^{2+\alpha}}\mathrm{d}t\right\} \tag{18}$$

Analogously the right Marchaud fractional derivative of $f'(x)$ reads:

$$D^{\alpha}_{b-}f'(x) = \frac{1}{\Gamma(1-\alpha)}\left\{\frac{f'(x)}{(b-x)^{\alpha}} + \alpha f'(x)\int_x^b \frac{\mathrm{d}t}{(t-x)^{1+\alpha}} + \alpha\lim_{t\to x^+}\left[\frac{f(t)-f(x)}{(t-x)^{1+\alpha}}\right] - \alpha\frac{f(b)-f(x)}{(b-x)^{1+\alpha}} + \alpha(1+\alpha)\int_x^b \frac{f(x)-f(t)}{(t-x)^{2+\alpha}}\mathrm{d}t\right\} \tag{19}$$

It must be observed that the expressions (18) and (19) are only formal since the second, the third and the fifth contributions at the right hand sides are divergent. Nevertheless, it can be easily checked that, subtracting Eq. (19) from Eq. (18), the first three terms disappear, so that:

$$D^{\alpha}_{a+}f'(x) - D^{\alpha}_{b-}f'(x) = \frac{\alpha}{\Gamma(1-\alpha)}\left[\frac{f(b)-f(x)}{(b-x)^{1+\alpha}} - \frac{f(x)-f(a)}{(x-a)^{1+\alpha}} + (1+\alpha)\int_a^b \frac{f(t)-f(x)}{|t-x|^{2+\alpha}}\mathrm{d}t\right] \tag{20}$$

Recalling the definition of Riemann–Liouville (3–5) and Caputo fractional derivatives (9–10) together with their relationships (12), the terms at the left hand side can be written as:

$$D^{\alpha}_{a+}f'(x) = DI^{1-\alpha}_{a+}f'(x) = D\,{}_{C}D^{\alpha}_{a+}f(x) = D^{1+\alpha}_{a+}[f(x)-f(a)] \tag{21a}$$

$$D^{\alpha}_{b-}f'(x) = -DI^{1-\alpha}_{b-}f'(x) = D\,{}_{C}D^{\alpha}_{b-}f(x) = -D^{1+\alpha}_{b-}[f(x)-f(b)] \tag{21b}$$

Due to linearity of the fractional derivative, we can split the computation of the right hand sides of Eqs. (21). Thanks to Eqs. (6) and (7), the fractional derivative of the constant parts can be directly computed: they cancel each other with the corresponding terms at the right hand side of Eq. (20). Recalling also the Gamma function property according to which $-\alpha\ \Gamma(-\alpha) = \Gamma(1-\alpha)$, Eq. (20) becomes:

$$D^{1+\alpha}_{a,b}f(x) = \frac{1}{2}\left[D^{1+\alpha}_{a+}f(x) + D^{1+\alpha}_{b-}f(x)\right] = \frac{1}{2\,\Gamma(-\alpha)}\left[\frac{f(x)}{(x-a)^{1+\alpha}} + \frac{f(x)}{(b-x)^{1+\alpha}} + (1+\alpha)\int_a^b \frac{f(x)-f(t)}{|x-t|^{2+\alpha}}\mathrm{d}t\right] \tag{22}$$

which is the results we were looking for: the Riesz derivative is now expressed by an integral where the difference $f(x) - f(t)$ appears. Quite surprisingly, if we set $\beta = 1 + \alpha$ (and hence $1 < \beta < 2$), Eq. (22) becomes:

$$D^{\beta}_{a,b}f(x) = \frac{1}{2\,\Gamma(1-\beta)}\left[\frac{f(x)}{(x-a)^{\beta}} + \frac{f(x)}{(b-x)^{\beta}} + \beta\int_a^b \frac{f(x)-f(t)}{|x-t|^{1+\beta}}\,\mathrm{d}t\right] \tag{23}$$

i.e. it coincides with the sum of Eqs. (14a) and (14b), which, taken separately, hold only for $0 < \beta < 1$. It means that, while the Marchaud definition of fractional derivative is given only for order of derivation lower than unity, its sum, i.e. the Riesz derivative, can be given in the Marchaud form for orders of fractional derivation up to 2. In other words, Eq. (23) holds true on the whole interval $0 < \beta < 2$.

This result will prove useful in Sect. 4. We conclude this section observing that the Riesz derivative (23) of the function f is equal to f, 0 and f'' when β is equal to 0, 1, 2, respectively. The fact that it vanishes for $\beta = 1$ (and, more generally for any odd number) is a consequence of the rule stating that the fractional derivative is equal to the opposite of the corresponding integer derivative when the order of derivation is an odd number, as noted previously.

3 Eringen and fractional nonlocal elasticity

In the present section, we will introduce a nonlocal elastic model that makes use of fractional calculus: we will name it *fractional nonlocal elasticity*. For the sake of simplicity we will deal only with the one-dimensional case. Furthermore, we start with a brief summary of integral nonlocal elasticity, aiming to highlight analogies and differences between the two approaches.

Nonlocal elasticity dates back to Kröner [31], who formulated a continuum theory with longe-range interactions. However, the most important contribution is due to Eringen. According to Eringen [32], the integral nonlocal elasticity theory differs from the standard local one in the stress–strain constitutive relation only: the stress σ at a point x of a bar depends on the strain field ε all over the bar by means of an attenuation function g. In formulae:

$$\sigma(x) = E\int_l g(t-x)\,\varepsilon(t)\mathrm{d}t \tag{24}$$

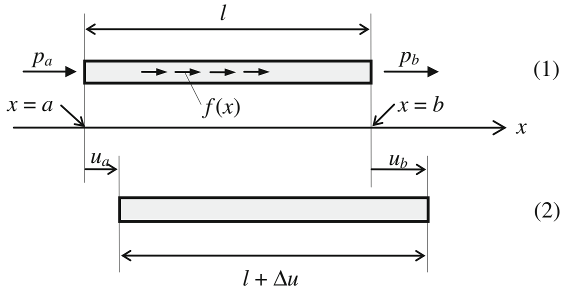

Fig. 1 Static (1) and kinematic (2) schemes for a bar under axial loads and displacements

where E is Young's modulus and l the bar length. On the other hand the equilibrium and kinematic equations remain standard, i.e. $\mathrm{d}\sigma/\mathrm{d}x + f(x) = 0$ and $\varepsilon = \mathrm{d}u/\mathrm{d}x$, respectively, where f is the external (axial) load per unit volume and u the longitudinal displacement (see Fig. 1).

The material stress response $\sigma(x)$ is defined as *nonlocal*, since it is expressed as a weighted value of the strain field over the whole bar length l. The attenuation function g defines how much the strain in t (the source points) affects the stress in x (the field points) and it is a function of their distance $r = t - x$. It is non-negative and it decays with $|r|$, i.e. $g(r) \to 0$ as $|r| \to \infty$, becoming null or negligible when r is larger than a characteristic material length l_{ch}, named the influence distance, usually much smaller than the bar length l.

It is worth observing that the regularity of the nonlocal stress field is not governed by the strain field alone, but also by the attenuation function. A consequence of this feature is that the stress singularities rising in local elasticity when dealing with cracked or notched geometries disappear when the same geometries are faced by means of nonlocal elasticity, thus allowing the use of stress-based failure criteria. This makes nonlocal elasticity very attractive for engineering purposes.

The distance r can be regarded as large or small only with respect to the material parameter l_{ch}. When this parameter tends to zero, the attenuation function is everywhere null except in x. It means that the attenuation function coincides with the Dirac function $\delta(x)$; in such a case nonlocal elastic constitutive Eq. (24) reverts to the local elastic one: $\sigma(x) = E\,\varepsilon(x)$.

Since the aim of the nonlocal relation (24) is to take into account the effect of a (varying) strain field in a neighbourhood of a given point on the stress in that point, it seems reasonable to require that, if the strain field is uniform, no differences must be observed with respect to the local elastic model. It is straightforward to observe that this goal is easily achieved by requiring that the area subtended by the attenuation function is equal to unity [33]:

$$\int_{-\infty}^{+\infty} g(r)\,\mathrm{d}r = 1 \tag{25}$$

Different kinds of attenuation functions can be implemented. Among the others, one may choose to use the Gaussian function, the bell-shaped function or the cone function, see Fig. 2a. For the sake of comparison with the fractional model, we will consider only the last case, which, in the one-dimensional version, reads:

$$g(r) = \begin{cases} \dfrac{1}{l_{\mathrm{ch}}}\left(1 - \dfrac{|r|}{l_{\mathrm{ch}}}\right) & \text{for } |r| \le l_{\mathrm{ch}} \\ 0 & \text{for } |r| > l_{\mathrm{ch}} \end{cases} \tag{26}$$

where the factor outside the round bracket has been chosen in order to fulfil Eq. (25). Equation (26) is plotted in Fig. 3a for different values of l_{ch}.

For a bar of infinite length, it is easy to provide a formulation where no spatial derivative of the displacement (i.e. no strain) appears. It is sufficient to integrate by parts Eq. (24) to get:

$$\sigma(x) = -E \int_{-\infty}^{+\infty} [u(t) - u(x)]\, g'(t-x)\,\mathrm{d}t \tag{27}$$

where the prime denotes derivation of the attenuation function g with respect to its argument $r = t - x$. Substitution of Eq. (27) into the equilibrium equation yields:

$$E \int_{-\infty}^{+\infty} [u(t) - u(x)]\, g''(t-x)\,\mathrm{d}t + f(x) = 0 \tag{28}$$

As will be emphasized in the next section, Eq. (28) allows one to interpret the nonlocal elastic model described by Eq. (24) as a material model characterized by long-range interactions between non-adjacent points represented by elastic springs of stiffness proportional to $E\ g''$. Equation (28) represents the basis of the peridynamics theory [34, 35], which looks particularly interesting since, avoiding the use of the strain, it can deal with non-smooth or discontinuous displacement fields.

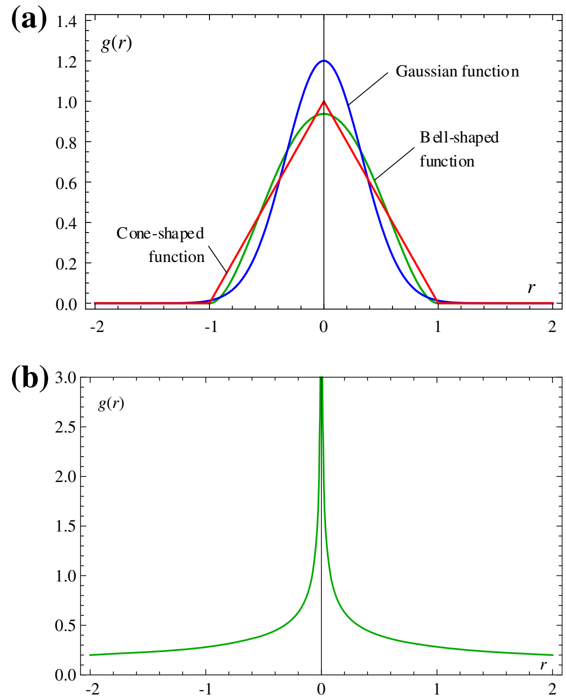

Fig. 2 Typical choices for the attenuation functions in nonlocal elasticity (**a**): cone-shaped function (*red*), bell-shaped function (*green*), Gaussian function (blue). Power law attenuation function for fractional nonlocal elasticity (**b**). (Color figure online)

Before introducing the fractional analogue to Eq. (24), it is worth observing that Eq. (24) represents the *integral* (or strong) nonlocality. We can develop in Taylor series the strain at point x.

$$\varepsilon(t) = \varepsilon(x) + \varepsilon'(x)\,(t-x) + \varepsilon''(x)\,\frac{(t-x)^2}{2} + \cdots \tag{29}$$

If we truncate the series at the quadratic term, substitute Eq. (29) into Eq. (24) and perform the integration (on an infinite domain, as above), we get:

$$\sigma(x) = E\left[\varepsilon(x) + \frac{l_{\mathrm{ch}}^2}{12}\varepsilon''(x)\right] \tag{30}$$

which represents the basis of the *gradient* (or weak) nonlocal theories. Note that the numerical value of the term multiplying the second derivative of the strain in

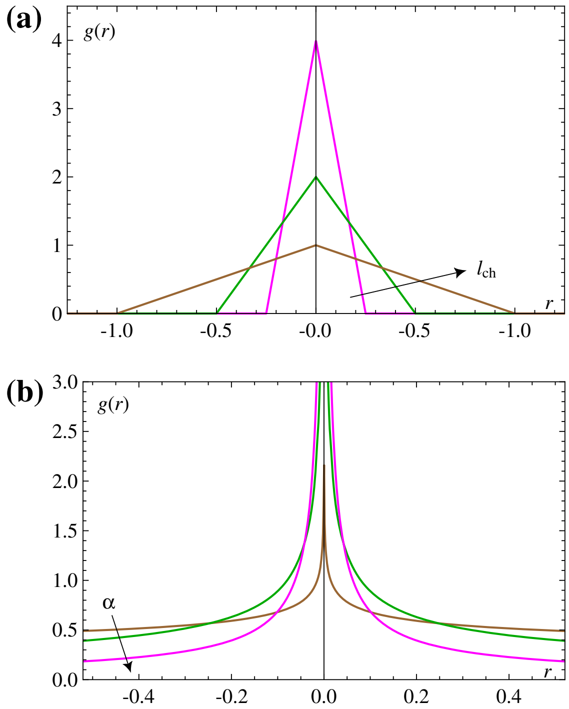

Fig. 3 Cone attenuation functions (**a**) for l_{ch} (in some linear measure) equal to 1 (*brown*), 0.5 (*dark green*), 0.25 (*magenta*). Power law attenuation functions (**b**) for α equal to 0.2 (*brown*), 0.5 (*dark green*), 0.8 (*magenta*). (Color figure online)

Eq. (30) depends on the shape of the attenuation function and it has been computed here assuming a conical shape according to Eq. (26). The results is however general, in the sense that in gradient elasticity the second derivative is multiplied by a material parameter with the physical dimension of a square length (see e.g. [36, 37]).

Let us now assume as attenuation function a power law, and, more in detail, the following expression:

$$g(r) = \frac{1}{2\,\Gamma(1-\alpha)\;|r|^{\alpha}} \tag{31}$$

with $0 < \alpha < 1$. Equation (31) is plotted in Fig. 2b for $\alpha = 0.5$ and for different values of α in Fig. 3b. As Fig. 3b points out, the main difference with respect to the commonly used attenuation functions is that the power law attenuation functions (31) are singular (but integrable) at $r = 0$ (i.e. $t = x$) and characterized by long tails for large r, whereas the standard ones are not singular in the origin and are null or rapidly vanishing for r values larger than l_{ch}. However, Fig. 3 shows also that both the power law and cone (as representative of the standard ones) attenuation functions change from smooth, weighing the strain on a wide range, to sharp, taking the strain in a narrow region into account: the parameter ruling this transition is the characteristic length l_{ch} for the cone function (or similar) and the exponent α for the power law.

Note that the radial coordinate in Eq. (31) could have been normalized with respect to a material length l_{ch} (as done for the cone function, see v(26)). In such a case we have the simultaneous presence of two parameters (α and l_{ch}) describing the transition between local and nonlocal behaviours. For a first attempt in this direction see [38].

It is worth observing that the physical dimensions of the attenuation functions (26) and (31) are different, being $[\mathrm{L}]^{-1}$ for Eq. (26) and $[\mathrm{L}]^{-\alpha}$ for Eq. (31). It means that Eq. (31) can still be substituted into Eq. (24), but the Young modulus E of the material must be replaced by a material parameter E^* (the fractional Young modulus) with anomalous physical dimension $[\mathrm{F}][\mathrm{L}]^{\alpha-3}$:

$$\sigma(x) = \frac{E^*}{2\,\Gamma(1-\alpha)} \int_a^b \frac{\varepsilon(t)}{|t-x|^{\alpha}}\,\mathrm{d}t \tag{32}$$

Denoting by a and b the extreme abscissas of the bar (of length $l = b - a$), it is easy to recognize the presence of the fractional Riesz integral (15a), so that Eq. (32) turns into:

$$\sigma(x) = E^* I^{1-\alpha}_{a,b}\,\varepsilon(x) \tag{33}$$

Although Eq. (33) could be seen as a special case of Eq. (24) (up to the substitution of E with E^*), since there is no characteristic length in Eq. (33) we prefer to distinguish the two models: thus Eq. (33) represents the constitutive equation of the one-dimensional *fractional* nonlocal elasticity, whereas Eq. (24) will be referred to as the material law characterizing *Eringen* nonlocal elasticity. Note that the Riesz integral in Eq. (33) ensures that the power law attenuation function (31) tends the Dirac function when $\alpha \to 1$ and, correspondingly, the fractional constitutive Eq. (33) reverts to its standard local counterpart $\sigma = E\,\varepsilon$ when α is equal to unity. On the other hand, as observed above, in Eringen nonlocal elasticity the local case is recovered by letting the characteristic length l_{ch} vanish.

The other limit is represented by the case $\alpha = 0$. In such a case, the attenuation function (31) turns out to be constant (and equal to 1/2). It means that the stress depends on the strain at any point of the bar in the same way, so that the dependence on x is lost. The fractional integral in Eq. (33) becomes a simple integral of the strain; hence the nonlocal stress is constant and everywhere equal to:

$$\sigma(x) = \sigma = \frac{E^*}{2}[u(b) - u(a)] = \frac{E^*}{2}\Delta u \tag{34}$$

Since the stress is proportional to the difference between the displacements of bar edges, we can also state that for $\alpha = 0$ the nonlocal elastic bar is equivalent to a spring connecting the bar extremes with stiffness $E^*/2$ (note that now the physical dimension of E^* are $[F][L]^{-3}$). A similar behaviour in Eringen nonlocal elasticity is obtained by letting l_{ch} tending to infinity.

In spite of several analogies between Eringen and fractional nonlocal elastic models, there are however some fundamental differences that we are now trying to point out. Let us consider, for instance, a bar subjected to a constant axial stress $\bar{\sigma}$ (i.e. $p_a = -\bar{\sigma}$, $p_b = +\bar{\sigma}, f \equiv 0$ in Fig. 1). According to Eringen and fractional nonlocal elasticity, respectively, the bar elongation Δu is a function of:

$$\Delta u = F(E, l, \bar{\sigma}, l_{ch}) \tag{35a}$$

$$\Delta u = F(E^*, l, \bar{\sigma}, \alpha) \tag{35b}$$

where, for the sake of simplicity, F denotes a generic functional dependence and not a specific function. A straightforward application of dimensional analysis and of linearity of the static, kinematic and constitutive equations leads to the following results:

$$\Delta u = F(\lambda) \times \frac{\bar{\sigma}}{E} l \tag{36a}$$

$$\Delta u = F(\alpha) \times \frac{\bar{\sigma}}{E^*} l^{\alpha} \tag{36b}$$

with $\lambda = l_{ch}/l$. Equation (36a) shows that, for the Eringen model and for a given λ value, the elongation is proportional to the bar length. More in detail, Δu tends to the local elastic value $\bar{\sigma}l/E$ if the bar is sufficiently long (i.e. $l \gg l_{ch}$), since the condition represented by Eq. (25) ensures that $f(\lambda) \to 1$ when $\lambda \to 0$.

On the other hand, Eq. (36b) shows that, for the fractional model, the elongation is proportional to the bar length raised to α. It means that, in order to have an average constant strain $\Delta u/l$, the stress must diverge as $l^{1-\alpha}$. This result is tantamount to observe that condition (25) can never be achieved in fractional nonlocal elasticity: no multiplicative factor can be given to the power law attenuation function $g(r)$ in order to ensure the fulfilment of Eq. (25). The analytical reason is simply that Eq. (31) is not integrable for $r \to \pm\infty$ and, correspondingly, the integral (25) diverges.

Equation (36b) shows also that the stiffness of a fractional bar decreases as $l^{-\alpha}$ ($0 < \alpha < 1$) instead of the standard result l^{-1}, holding both for local and nonlocal Eringen elasticity (provided that $l \gg l_{ch}$). While this different scaling marks a difference between the fractional and Eringen models, here it is worth noting that this scaling property represents a contact point with those models where strain concentrates on fractal subsets. The interested reader is referred to the paper by Carpinteri et al. [8] where the Cantor bar model was outlined, proving that the elongation scales as l^{α}, α being the non-integer dimension of the fractal set representing the deformable region of the bar. Thus, although the origin is quite different, the fractional nonlocal model and fractal local model are characterized by the same scaling properties. For a review on the relations between fractal and fractional calculus see also [39].

While the strain field associated to a constant stress need the numerical solution of a fractional differential equation to be computed and its analysis is therefore postponed in the following sections, the computation of the stress field generating a constant strain $\bar{\varepsilon}$ is just a matter of integration. According to Eringen nonlocal elasticity (by means of a conical attenuation function) and to fractional nonlocal elasticity, the stress fields read, respectively (assuming $a = 0$ and $b = l$):

$$\sigma(x) = \begin{cases} \dfrac{E\bar{\varepsilon}}{2}\left[1 + 2\dfrac{x}{l_{ch}} - \left(\dfrac{x}{l_{ch}}\right)^2\right], & \text{for } 0 < x < l_{ch}, \\ E\bar{\varepsilon}, & \text{for } l_{ch} < x < l - l_{ch}, \\ \dfrac{E\bar{\varepsilon}}{2}\left[1 + 2\dfrac{(l-x)}{l_{ch}} - \left(\dfrac{l-x}{l_{ch}}\right)^2\right], & \text{for } l - l_{ch} < x, \end{cases} \tag{37a}$$

$$\sigma(x) = \frac{E^* l^{1-\alpha}}{2\Gamma(2-\alpha)}\,\bar{\varepsilon}\left[\left(\frac{x}{l}\right)^{1-\alpha} + \left(1 - \frac{x}{l}\right)^{1-\alpha}\right] \tag{37b}$$

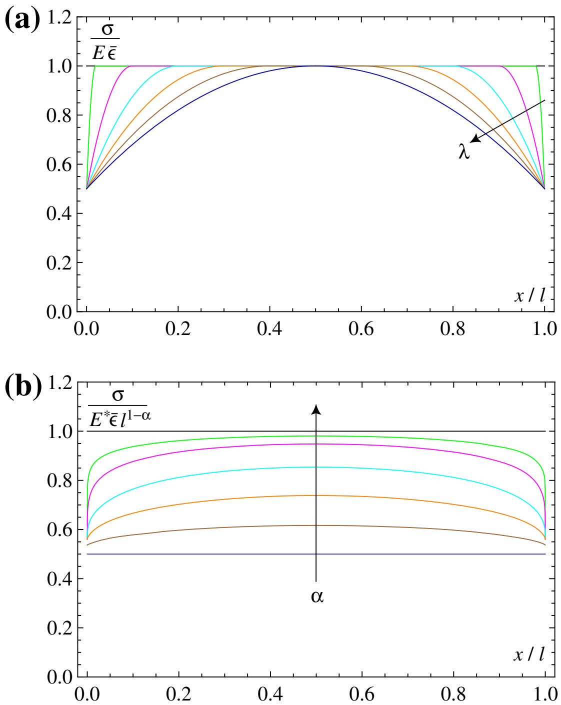

Fig. 4 Stress field for a uniformly stretched bar: nonlocal elastic solution (with cone attenuation function) for $\lambda = l_{ch}/l$ equal to 0.5, 0.4, 0.3, 0.2, 0.1, 0.02 from the *dark blue line* to the green one (**a**); fractional nonlocal elastic solution for α equal to 0, 0.2, 0.4, 0.6, 0.8, 0.9 from the *dark blue line* to the green one (**b**). The black, constant, unit function represents the standard local-elastic solution to which both the families of curves tend through a non-uniform convergence (for $\lambda \to 0$ and $\alpha \to 1$, respectively) . (Color figure online)

which are plotted in Fig. 4a and b for different $\lambda = l_{ch}/l$ and α values, respectively. It is evident that, for both Eringen and fractional nonlocal elasticity (i.e. for both Eq. (24) and (33)) the stress is lower at the edges for any value of the parameters. This peculiar behaviour is due to the boundary effect: in the points close to the border there is "less" strain to affect the nonlocal stress and, consequently, the external regions of the bar are less stiff. The two solutions (37a) and (37b) are similar under many aspects: (i) they both tend to the local solution $\sigma = E\,\varepsilon$, when $\lambda \to 0$ and $\alpha \to 1$ respectively; (ii) for small λ values and α values close to 1, both the solutions show a boundary layer where the stress sharply decreases, whereas in the central portion of the bar the strain is (approximately) constant; (iii) for relatively large λ values (i.e. approaching unity) and α close to 0, the stress field tend to be rather smooth since the strain is averaged over almost the whole bar.

Although very similar under many respects, the two models have two substantial differences. The former one is that Eringen model coincides with the local solution at a certain distance from the borders, whereas the fractional model does not because of the long tails of the power law attenuation function. Thus we can say that the fractional model shows a stronger nonlocality, which affects the whole structure although decaying from the source points (in this case the borders). The latter one is that the two models strongly deviate for what concerns the dependence on the bar length, as already outlined by the previous dimensional analysis. According to Eringen model, the effect of a length increment is the relative narrowing of the boundary layer, whose absolute size remains unchanged since it is related to the material length l_{ch}. As evident in Fig. 4a, the overall shape of the stress field changes accordingly, while the nonlocal stress values do not vary. The opposite occurs for the fractional model: varying the bar length has no effect on the shape of the stress field since it depends only on the exponent α; hence the absolute size of the boundary layer scales with the bar length. On the other hand, Eq. (37b) clearly shows that the whole stress field increases along with the bar length as $l^{1-\alpha}$.

We thus conclude this preliminary comparison between Eringen and fractional nonlocal elastic models observing that they present several analogies, but also some different features that probably make them applicable to different classes of materials. While the former model seems to be more effective in describing materials where the nonlocal effects soften beyond a certain material length, the latter seems to be more suitable to deal with materials where the nonlocal interactions affect the overall mechanical behaviour, giving rise to non-standard, power law size effects.

We conclude the present section providing some alternative expressions to the fractional nonlocal constitutive Eq. (33). For instance, we can imagine a material whose constitutive law is the sum of a local term plus a fractional nonlocal one. In such a case the material stress–strain relationship reads:

$$\sigma(x) = \beta_1 E \varepsilon(x) + \beta_2 E^* I^{1-\alpha}_{a,b} \varepsilon(x) \qquad (38)$$

where β_1 and β_2 are two numerical coefficients. If one chooses $\beta_1 + \beta_2 = 1$, Eq. (38) can be interpreted as the constitutive equation of a two-phase elastic material, where the first phase obeys to a local elasticity, whereas the second phase obeys to fractional nonlocal elasticity. As for Eq. (33), also the material law (38) reverts to the local elastic relation $\sigma = E\,\varepsilon$ when $\alpha \to 1$. Equation (38) has been used in [19] to analyze wave propagation in fractional nonlocal elastic media.

The ratio of the fractional Young modulus E^* to the Young modulus E is a material parameter with the physical dimension of a length raised to $(\alpha - 1)$. Therefore we can indicate such a ratio with $l_{\text{ch}}^{\alpha-1}$. Accordingly, if we now choose $\beta_1 = \beta_2 = 1$, Eq. (38) becomes:

$$\sigma(x) = E\left[\varepsilon(x) + l_{\text{ch}}^{\alpha-1}\, I_{a,b}^{1-\alpha}\varepsilon(x)\right] \tag{39}$$

which was the form proposed in [16]. The expression given in Eq. (39) seems particularly attractive since it can describe synthetically a variety of material laws. Although in the present paper we have provided a physical meaning to Eq. (39) only in the range $0 < \alpha < 1$, we could consider α values external to the range (0,1). In [14] a fractional model was developed that corresponds to α values in the range $(-1,0)$. However, in the present context, such a choice does not show a clear mechanical meaning, since it corresponds to a function $g(r)$ (see Eq. (31)) monotonically increasing and therefore being no more an "attenuation" function. On the other hand, noting that negative fractional order integrals correspond to fractional derivative, in our opinion it would be more interesting to consider α values in the range (1,3) since, for the limit case $\alpha = 3$, Eq. (39) reverts to Eq. (30), i.e. to the well-known gradient elasticity [36]. The fractional model corresponding to Eq. (39) with $0 < \alpha < 3$ could hence be the key to relate integral and gradient nonlocal elasticities, as also the preliminary results by Tarasov [23] seem to indicate (see also [20]). However, for the sake of simplicity, in the following sections we will consider only the constitutive law (33) in the range (0,1), letting the analyses of different fractional order values to future works.

4 Fractional nonlocal elastic bar

In the present section we will provide the governing equation in term of the longitudinal displacement for a bar made of a material obeying the constitutive Eq. (33) under static loads (Fig. 1). We will refer to such a model as the *fractional nonlocal elastic bar*. Furthermore it will be proved that the fractional nonlocal elastic bar can be seen as the continuum limit of a lattice model.

Since the strain ε is the spatial derivative of the displacement u, recalling Caputo definitions of forward and backward fractional derivatives, it is straightforward to express the nonlocal stress (33) as a function of the displacement. It reads:

$$\sigma(x) = \frac{E^*}{2}\left[{}_{\text{C}}D_{a+}^{\alpha}u(x) \; - {}_{\text{C}}D_{b-}^{\alpha}u(x)\right] \tag{40}$$

Note that the property that Caputo fractional derivative of a constant is zero (see Sect. 2) guarantees that a rigid body displacement does not affect the stress field. By means of Eqs. (14), we can give the nonlocal stress the following expression:

$$\sigma(x) = \frac{E^*}{2\,\Gamma(1-\alpha)}\left[\frac{u(x)-u(a)}{(x-a)^{\alpha}} + \frac{u(b)-u(x)}{(b-x)^{\alpha}} + \alpha\int_a^b \text{sign}(x-t)\,\frac{u(x)-u(t)}{|x-t|^{1+\alpha}}\text{d}t\right] \tag{41}$$

where no derivatives of the displacement appear. Equation (41) represents the fractional counterpart, for a bar of finite length, of Eq. (27), holding for an infinite Eringen bar.

By means of Eqs. (12), the Caputo fractional derivatives in Eq. (40) can be replaced by the Riemann–Liouville ones. Then, substitution of Eq. (40) into the equilibrium equation $\text{d}\sigma/\text{d}x + f(x) = 0$ yields:

$$\frac{E^*}{2}\left\{D_{a+}^{1+\alpha}[u(x)-u(a)] \; + D_{b-}^{1+\alpha}[u(x)-u(b)]\right\} + f(x) = 0 \tag{42}$$

Note that Eq. (42) can be also written in terms of the strain by directly substituting Eq. (33) into the equilibrium equation, leading to:

$$\frac{E^*}{2}\left[D_{a+}^{\alpha}\varepsilon(x) \; - \; D_{b-}^{\alpha}\varepsilon(x)\right] + f(x) = 0 \tag{43}$$

Exploiting the linearity of the fractional derivatives, it is easy to recognize the presence of the Riesz derivative (15b) in Eq. (42). Formulae (6–7) provide (also) the fractional derivative of a constant, so that Eq. (42) turns into:

$$D_{a,b}^{1+\alpha}u(x)+\frac{\alpha}{2\Gamma(1-\alpha)}\left[\frac{u(a)}{(x-a)^{1+\alpha}}+\frac{u(b)}{(b-x)^{1+\alpha}}\right]+\frac{f(x)}{E^*}=0 \tag{44}$$

which represents the fundamental equation of the fractional nonlocal bar. Equation (44) is a fractional differential equation of order comprised between 1 and 2; as such, it needs two boundary conditions [1] to be integrated. Provided that at least one of them is a kinematic one in order to avoid rigid body displacement, at each edge boundary conditions can be either kinematic or static. Hence, in $x=a$ and in $x=b$, we have, respectively:

$$u(a)=u_a \quad \text{or} \quad \sigma(a)=-p_a \tag{45a}$$

$$u(b)=u_b \quad \text{or} \quad \sigma(b)=p_b \tag{45b}$$

where p_a and p_b are the external longitudinal forces per unit of cross sectional area acting at the edges. The minus sign in Eq. (45a) is because we assume positive p if directed along the x axis (see Fig. 1). Aiming to integrate Eq. (44), static boundary conditions must be expressed in terms of the displacement function. This goal is readily achieved by means of Eq. (40); they read:

$${}_{\mathrm{C}}D_{b-}^{\alpha}u\big|_{x=a}=-\frac{1}{\Gamma(1-\alpha)}\int_a^b\frac{u'(t)}{(t-a)^{\alpha}}\mathrm{d}t=\frac{p_a}{E^*/2} \tag{46a}$$

$${}_{\mathrm{C}}D_{a+}^{\alpha}u\big|_{x=b}=\frac{1}{\Gamma(1-\alpha)}\int_a^b\frac{u'(t)}{(b-t)^{\alpha}}\mathrm{d}t=\frac{p_b}{E^*/2} \tag{46b}$$

that is, static boundary conditions are integral conditions imposing the value of the backward Caputo derivative in the left extreme and of the forward Caputo derivative in the right extreme, respectively.

It is worth noting that, as for the constitutive Eq. (33), in the fractional differential Eq. (44) $0<\alpha<1$. While for $\alpha\to 1$ the equation tends to the local elastic equation $E\ u''+f=0$ (note that $\Gamma(0)=\infty$), for $\alpha=0$ and $f(x)\neq 0$ Eq. (33) admits no solution. From an analytical point of view, the reason is that the Riesz derivative of order one is zero. From a physical point of view, we have already seen that for $\alpha=0$ the nonlocal bar collapses on a spring connecting its extremes (see Eq. (34)) and, accordingly, it can withstand only external loads applied at its edges. In order to avoid this anomalous behaviour, it is sufficient to retain a local elastic contribution in the constitutive law, as provided, for instance, by Eq. (38) or (39). However, for the sake of simplicity and wishing to consider α values close to unity (i.e. small deviations from standard local elasticity), we will keep on using the material law (33) and the corresponding fractional differential Eq. (44).

In order to solve the mathematical problem represented by the fractional differential Eq. (44) and the proper boundary conditions (45–46), a suitable numerical technique is needed even for simple load functions. The numerical analysis will be given in the next section. Here we want to provide a further mechanical interpretation to Eqs. (44–46) in terms of a lattice model. This goal is readily achieved by exploiting the result of the proof given in Sect. 2 which provides a suitable expression of the Riesz derivative of order up to 2. Thus, substituting Eq. (22) into Eq. (44) (or, more directly, substituting Eq. (20) into Eq. (43)) yields:

$$\frac{\alpha}{2\Gamma(1-\alpha)}\left[\frac{u(b)-u(x)}{(b-x)^{1+\alpha}}-\frac{u(x)-u(a)}{(x-a)^{1+\alpha}}+(1+\alpha)\int_a^b\frac{u(t)-u(x)}{|x-t|^{2+\alpha}}\mathrm{d}t\right]+\frac{f(x)}{E^*}=0 \tag{47}$$

Equation (47) represents the fractional counterpart, for a bar of finite length, of the equilibrium Eq. (28) of a peridynamic bar of infinite length: notice that no spatial derivatives of the displacement appear in such a formulation. Accordingly, static boundary conditions (46) must be expressed as (by means of Eqs. (14)):

$$\frac{-1}{\Gamma(1-\alpha)}\left[\frac{u(b)-u(a)}{(b-a)^{\alpha}}+\alpha\int_a^b\frac{u(t)-u(a)}{(t-a)^{1+\alpha}}\mathrm{d}t\right]=\frac{p_a}{E^*/2} \tag{48a}$$

$$\frac{1}{\Gamma(1-\alpha)}\left[\frac{u(b)-u(a)}{(b-a)^{\alpha}}+\alpha\int_a^b\frac{u(b)-u(t)}{(b-t)^{1+\alpha}}\,\mathrm{d}t\right]=\frac{p_b}{E^*/2} \tag{48b}$$

In the form given by Eqs. (47) and (48) it is evident that the fractional nonlocal bar is the continuum limit of a discrete lattice model. To highlight the equivalence between the models, it is sufficient to write Eqs. (47–48) in discrete form. To this aim, we introduce a partition of the bar length $l = b - a$ in n ($n \in N$) intervals of length $\Delta x = l/n$. The generic point of the partition has abscissa x_i, with $i = 1,\ldots, n + 1$ and $x_1 = a$, $x_{n+1} = b$; u_i is the displacement at point x_i. For inner points (i.e. for $i = 2,\ldots, n$), the discrete form of Eq. (47) reads:

$$\frac{\alpha E^*}{2\Gamma(1-\alpha)}\left[-\frac{u_i-u_1}{(x_i-x_1)^{1+\alpha}}+\frac{u_{n+1}-u_i}{(x_{n+1}-x_i)^{1+\alpha}}+(1+\alpha)\sum_{\substack{j=1,\\ j\neq i}}^{j=n+1}\frac{u_j-u_i}{|x_j-x_i|^{2+\alpha}}\Delta x\right]+f_i=0 \tag{49}$$

while the static boundary conditions (48) holding at the outer points (i.e. for $i = 1$ and $i = n + 1$) read:

$$\frac{-E^*}{2\Gamma(1-\alpha)}\left[\frac{u_{n+1}-u_1}{(x_{n+1}-x_1)^{1+\alpha}}+\alpha\sum_{j=2}^{j=n+1}\frac{u_j-u_1}{|x_j-x_1|^{1+\alpha}}\Delta x\right]=p_a \tag{50a}$$

$$\frac{E^*}{2\Gamma(1-\alpha)}\left[\frac{u_{n+1}-u_1}{(x_{n+1}-x_1)^{1+\alpha}}+\alpha\sum_{j=1}^{j=n}\frac{u_{n+1}-u_j}{|x_{n+1}-x_j|^{1+\alpha}}\Delta x\right]=p_b \tag{50b}$$

Let us now introduce linear elastic spring elements, whose constitutive law is $p = k\ \Delta u$, where k is the spring stiffness, Δu is the relative displacement between the two points connected by the spring and p is the force (per unit of bar cross section area) acting at the same points. It is evident that we can interpret the nonlocal terms present in Eqs. (49–50) as long range interactions generated by linear elastic springs connecting non-adjacent material points. Hence Eqs. (49–50) can be rewritten as:

$$k^{ss}_{n+1,1}(u_{n+1}-u_1)+\sum_{j=2}^{j=n+1}k^{vs}_{j,1}(u_j-u_1)+p_a=0 \tag{51a}$$

$$-k^{vs}_{i,1}(u_i-u_1)+k^{vs}_{n+1,i}(u_{n+1}-u_i)+\sum_{j=1,j\neq i}^{j=n+1}k^{vv}_{j,i}(u_j-u_i)+p_i=0,\ \text{with}\ i=2,\ldots,n \tag{51b}$$

$$-k^{ss}_{n+1,1}(u_{n+1}-u_1)-\sum_{j=1}^{j=n}k^{vs}_{n+1,j}(u_{n+1}-u_j)+p_b=0 \tag{51c}$$

where $p_i = f_i\,\Delta x$ is the external force (per unit of cross section area) acting at point x_i; positive terms represents forces in the x direction and vice versa. Equations (51) represent the equilibrium equations for each material point ($i = 1,\ldots, n + 1$) in a nonlocal lattice whose points are connected by three sets of springs (see Fig. 5): the $n(n + 1)/2$ springs connecting the inner material points each other, describing the long range interactions between non-adjacent (and adjacent) volumes, whose stiffness is k^{vv}; the $(2n - 1)$ springs connecting the inner material points with the bar edges, ruling the volume-surface nonlocal interactions, with stiffness k^{vs}; the third set is represented by a unique spring connecting the bar edges, with stiffness k^{ss}, taking the surface–surface long-range interactions into account. Provided that the indexes are never equal one to the other, the following expressions for the stiffnesses hold ($i,j = 1,\ldots, n + 1$):

$$k^{vv}_{j,i}=\frac{\alpha(1+\alpha)E^*}{2\,\Gamma(1-\alpha)}\ \frac{(\Delta x)^2}{|x_j-x_i|^{2+\alpha}} \tag{52a}$$

$$k^{vs}_{n+1,i}=\frac{\alpha E^*}{2\,\Gamma(1-\alpha)}\ \frac{\Delta x}{(x_{n+1}-x_i)^{1+\alpha}}\ \text{and}\quad k^{vs}_{i,1}=\frac{\alpha E^*}{2\,\Gamma(1-\alpha)}\ \frac{\Delta x}{(x_i-x_1)^{1+\alpha}} \tag{52b}$$

$$k^{ss}_{1,n+1}=\frac{E^*}{2\,\Gamma(1-\alpha)}\ \frac{1}{(x_{n+1}-x_1)^{\alpha}} \tag{52c}$$

For the sake of clarity, the equivalent lattice model is drawn in Fig. 5 for $n = 4$.

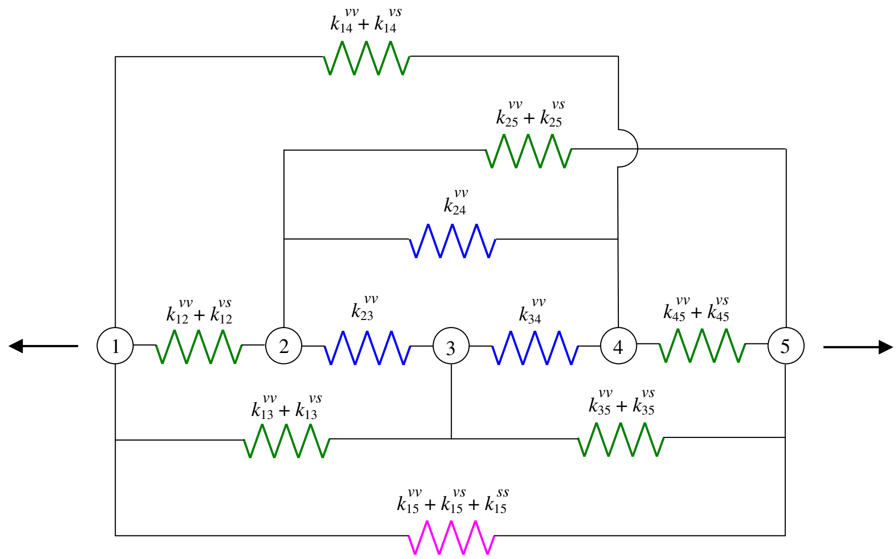

Fig. 5 Nonlocal lattice model equivalent to the nonlocal fractional elastic bar ($n = 4$). The three sets of springs are drawn in different colours: when the spring stiffness is given by the sum of more contributions, the colour is given by the dominant spring as $\Delta x \to 0$. (Color figure online)

Thus we have proven that the continuum model of a nonlocal elastic bar whose constitutive law is given by the fractional relationship (33) is equivalent, for $n \to \infty$, to a lattice model whose points are connected by three sets of springs ruling the nonlocal interactions. The stiffness of all the springs decay with the distance between the connected material points, although the decaying velocity is higher for the volume–volume interactions, intermediate for the volume-surface long-range forces and lower for the surface-surfaces ones; furthermore their absolute stiffness are proportional to $(\Delta x)^2$, Δx and $(\Delta x)^0$, respectively. However, since the most numerous are the springs with the faster decay (or vanishing more quickly as $\Delta x \to 0$) and vice versa, all the three sets of springs contribute to give the bar a stiffness decreasing with the length as $l^{-\alpha}$, so that its elongation (under a constant stress) scales with l^{α}, as already shown by dimensional analysis arguments (see Eq. (36b)).

If an infinite bar is considered, only the connections between inner points (given by Eq. (52a)) remain and a direct comparison with the peridynamics Eq. (28) is thus possible. In this respect, a nice feature (i.e. more significant from a physical point of view) of the present fractional model is that the intensities of the long-range forces decrease with the distance, whereas this monotonic behaviour is not always met for the general Eringen nonlocal elastic law (24). In fact the stiffness of the nonlocal springs are proportional to the second derivative of $g(r)$ (see Eq. (28)), which is non-monotonic in general, as it is evident if we choose the Gaussian function or the bell function as attenuation function (see Fig. 2a).

For what concerns the limit cases, when $\alpha \to 1$, the long-range interactions tend to zero: only local (i.e. between adjacent material points) interactions are retained (the Gamma function tends to infinity, but the integral in Eq. (47) diverges) and the model tends to a local elastic bar (i.e. a spring chain, each one with stiffness equal to $E^*/\Delta x$). The other limit case is $\alpha \to 0$: accordingly, the stiffnesses of first two sets of springs (Eqs. 52a and 52b) vanish. The model is thus equivalent to a unique spring connecting the bar extremes, whose stiffness (Eq. 52c) attains the value $E^*/2$. This result is coherent with the limit expression (Eq. 34) of the fractional constitutive law (Eq. 33).

We conclude this section noticing that in [14] a point-spring model with only one set of spring (i.e. the volume–volume ones) was proposed and analyzed. Actually Di Paola & Zingales [14] were the first to highlight the equivalence of fractional nonlocal models with point-spring models. However they considered a stiffness with a too slow decay (as $r^{-(1+\alpha)}$ instead of $r^{-(2+\alpha)}$, see Eq. (52a)): such a choice makes the overall bar stiffness increasing with the length (as $l^{1-\alpha}$) instead of decreasing, i.e. it yields a structural behaviour apparently lacking a clear physical meaning.

5 Numerical simulations

Despite the clear mechanical meaning provided by the equivalent lattice, the discretization (51) is not the most efficient way to solve the fractional differential Eq. (44). Particularly, it is not able to catch the solution for α approaching unity, when the singularity of the integrand function in Eq. (22) is particularly strong. Since the order of fractional derivation is comprised between 1 and 2 for the field Eq. (44) and between 0 and 1 for the static boundary conditions (46), here we propose a numerical scheme based on the so-called L1–L2 algorithms that can be found in [24, 40].

From Eqs. (13), it is to check that:

$$D_{a+}^{1+\alpha}[u(x)-u(a)] = {}_{C}D_{a+}^{1+\alpha}u(x) + \frac{u'(a)}{\Gamma(1-\alpha)(x-a)^{\alpha}} = \frac{1}{\Gamma(1-\alpha)}\left[\frac{u'(a)}{(x-a)^{\alpha}} + \int_a^x \frac{u''(t)}{(x-t)^{\alpha}}\mathrm{d}t\right] \quad (53a)$$

$$D_{b-}^{1+\alpha}[u(x)-u(b)] = {}_{C}D_{b-}^{1+\alpha}u(x) + \frac{u'(b)}{\Gamma(1-\alpha)(b-x)^{\alpha}} = \frac{1}{\Gamma(1-\alpha)}\left[-\frac{u'(b)}{(b-x)^{\alpha}} + \int_x^b \frac{u''(t)}{(t-x)^{\alpha}}\mathrm{d}t\right] \quad (53b)$$

By approximating the first and the second order derivatives by means of the usual finite differences and evaluating analytically the remaining part of the integrals in Eqs. (53) and (46), we get the following approximate discrete expressions of the fractional differential Eq. (42) along with its static boundary conditions (46):

$$\frac{E^*}{2\Gamma(2-\alpha)\Delta x^{\alpha}}\sum_{j=0}^{n-1}\left(u_{j+1}-u_{j+2}\right)\left[(j+1)^{1-\alpha}-j^{1-\alpha}\right] = p_a \quad (54a)$$

$$\frac{E^*}{2\Gamma(2-\alpha)\Delta x^{\alpha}}\left\{\frac{1-\alpha}{(i-1)^{\alpha}}(u_2-u_1) + \sum_{j=0}^{i-2}\left(u_{i-j+1}-2u_{i-j}+u_{i-j-1}\right)\left[(j+1)^{1-\alpha}-j^{1-\alpha}\right] - \frac{1-\alpha}{(n-i+1)^{\alpha}}(u_{n+1}-u_n) + \sum_{j=0}^{n-i}\left(u_{i+j+1}-2u_{i+j}+u_{i+j-1}\right)\left[(j+1)^{1-\alpha}-j^{1-\alpha}\right]\right\} + p_i = 0, \quad i = 2,\ldots,n \quad (54b)$$

$$\frac{E^*}{2\,\Gamma(2-\alpha)\,\Delta x^{\alpha}}\sum_{j=0}^{n-1}\left(u_{n-j+1}-u_{n-j}\right)\left[(j+1)^{1-\alpha}-j^{1-\alpha}\right] = p_b \quad (54c)$$

Equations (54) represent a linear system of $(n+1)$ equations in the u_i $(i = 1,\ldots, n+1)$ unknowns. The solution is unique up to a constant which represents the irrelevant rigid body displacement that can be avoided by substituting one of the static boundary conditions with the corresponding kinematic condition (see Eqs. (45)). With respect to Eqs. (51), Eqs. (54) are an alternative (and more efficient) way to solve numerically the fractional differential elastic problem represented by Eqs. (44–45).

The algorithm (54) is now implemented to solve some example problems in order to show the capabilities of the numerical technique and the basic features of the structural response provided by the fractional nonlocal model. Note that, in order to reduce the number of the parameters affecting the solution, dimensional analysis is applied for each case (as done for Eqs. (35–36)) and results are plotted in a proper, normalized form.

The first case we consider is the stretched bar geometry depicted in Fig. 6a. Since the stress is constant throughout the bar, this configuration is complementary to the case of uniform strain considered in Sect. 3 (see Fig. 4b). For what concerns the displacement field (Fig. 6b), we note small variations with respect to the local elastic case. Stronger variations are observed in the strain field. Figure 6c clearly shows that strain localizes at the bar extremes and the strain concentration increases as α departs from unity. This peculiar effect is a consequence of the nonlocality of the stress: according to Eq. (33), at the edges strain must increase in order to provide a constant stress throughout the bar. In other words, the boundaries are less stiff than the bulk region and this is also the reason why stress diminishes at the edges in the constant strain case considered in Fig. 4b. Finally it is worth observing that all the curves approximately intersect at the same points.

The second case is represented in Fig. 7a. The strain is assumed to be constant in both the bar halves, but opposite in sign. In such a case the stress can be recovered without solving the fractional differential equation: it is just a matter of integrating Eq. (33). The

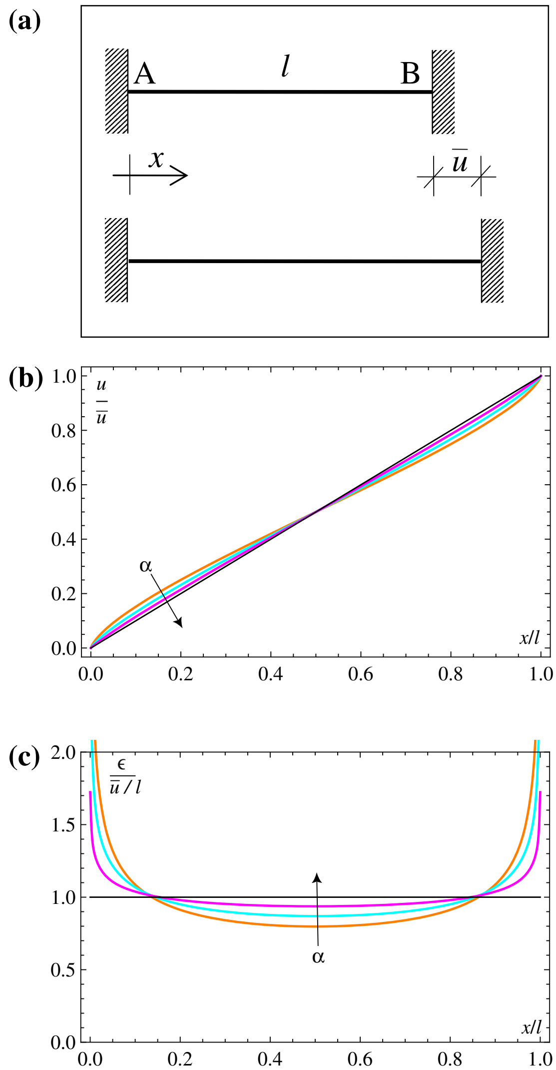

Fig. 6 Stretched fractional nonlocal elastic bar (**a**). Normalized displacement (**b**) and strain (**c**) fields for different fractional orders: $\alpha = 0.4$ (orange line), 0.6 (*cyan line*), 0.8 (*magenta line*), 1 (*black line*). Black lines correspond to standard local elasticity. (Color figure online)

result is plotted in Fig. 7b for different α values. It is evident the regularization effect on the stress field of the fractional nonlocal constitutive law: the stress jump at the mid-span characteristic of the local elastic solution ($\alpha = 1$) disappears for any α lower than unity. The stress field becomes smoother and smoother as α diminishes, finally tending to zero for $\alpha \to 0$, when the stress depends on the strain averaged over the whole bar length.

Somehow complementary to the previous case is that depicted in Fig. 8a, where the clamped–clamped

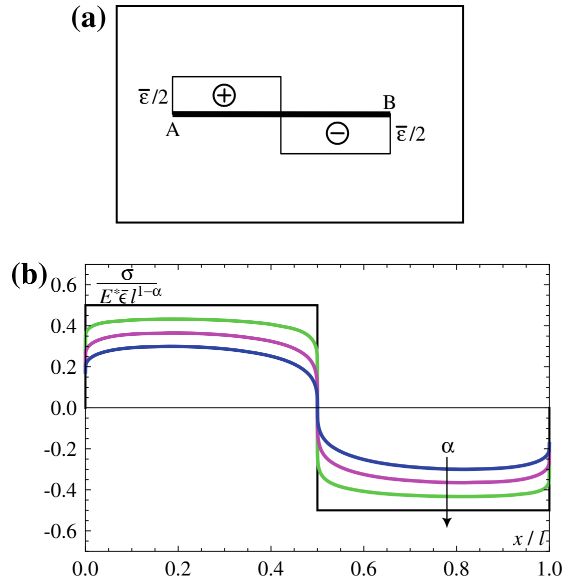

Fig. 7 Fractional nonlocal elastic bar under constant piecewise strain field (**a**). Normalized stress field (**b**) for different fractional orders: $\alpha = 0.7$ (*blue line*), 0.8 (*magenta line*), 0.9 (*green line*), 1 (*black line*). *Black line* corresponds to standard local elasticity. (Color figure online)

fractional nonlocal elastic bar is subjected to a concentrated axial force acting at the mid-span. Because of symmetry the stress field is known a priori, constant and opposite in the two halves. The algorithm (54) allows us to achieve the axial displacement (Fig. 8b) and strain (Fig. 8c) functions, properly normalized, for different α values: it is evident the departure from the linear and constant solutions (characteristic of a local elastic material). It is here worth emphasizing that what really matters is the shape of the solution and not its absolute value. In fact, since the physical dimensions of the fractional Young's modulus (entering the normalization factor, see Fig. 8b and 8c) vary along with α, an absolute comparison between the displacement/strain values related to different fractional order values is not significant.

Figure 8b shows that, for $\alpha < 1$, the displacement solution departs from the linearity characterizing the local-elastic case ($\alpha = 1$). This non-linear behaviour is higher at the boundaries (for what already observed) and at the mid-span, where the concentrated force acts. This effect is even higher if we consider the strain field plotted in Fig. 8c, where it is evident the strain

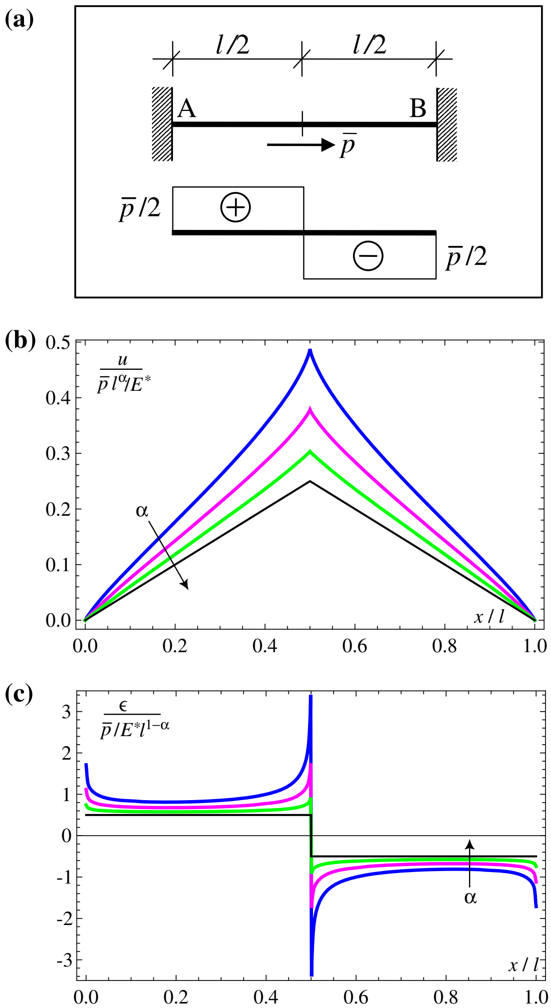

Fig. 8 Fractional nonlocal elastic bar with a longitudinal force at mid-span: stress field (**a**). Normalized displacement (**b**) and strain (**c**) fields for different fractional orders: $\alpha = 0.7$ (*blue line*), 0.8 (*magenta line*), 0.9 (*green line*), 1 (*black line*). Black lines correspond to standard local elasticity. (Color figure online)

localization at these points. A strain field more irregular than the stress one is not surprising: as observed for the previous case, the nonlocal law provides a regularization of the stress function starting from a given strain. Therefore, if the stress function is discontinuous (as in the present case, see Fig. 8a), the corresponding strain field must be even more irregular in the neighbourhood of the stress jump.

The fourth and last geometry considered is plotted in Fig. 9a. The left half is subjected to a uniformly distributed axial load. The displacement and strain

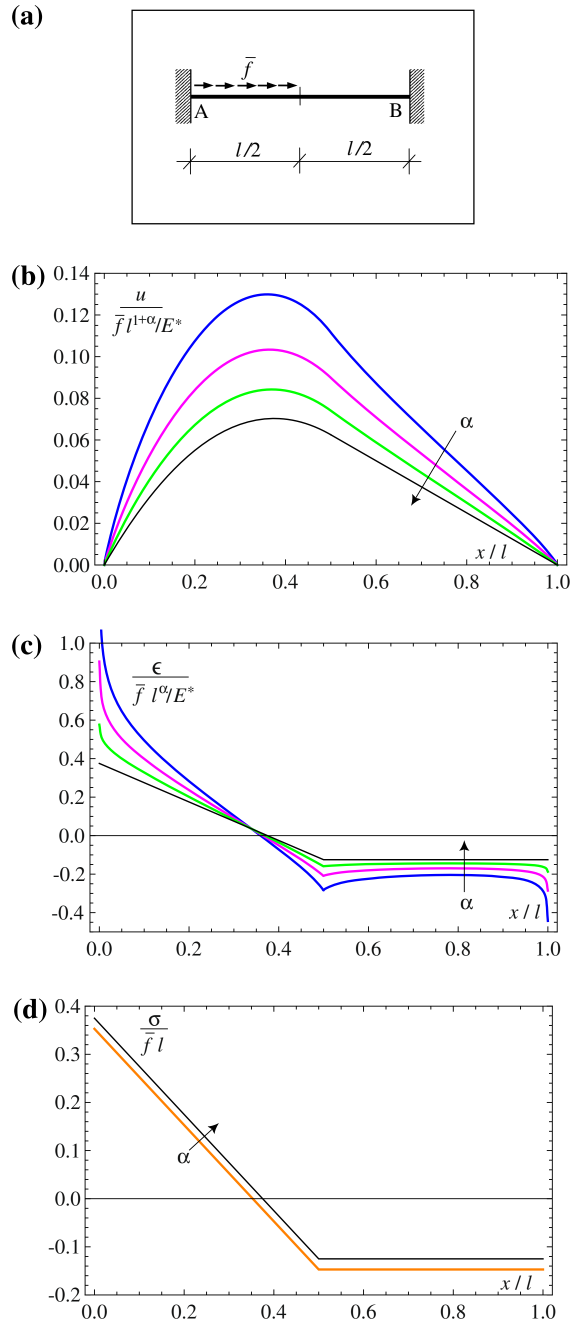

Fig. 9 Fractional nonlocal elastic bar with a uniformly distributed axial force on the left half (**a**). Normalized displacement (**b**) and strain (**c**) fields for different fractional orders: $\alpha = 0.7$ (*blue line*), 0.8 (*magenta line*), 0.9 (*green line*), 1 (*black line*). Normalized stress field (**c**) for $\alpha = 0.4$ (*orange line*) and 1 (*black line*). Black lines correspond to standard local elasticity. (Color figure online)

fields are plotted in Figs. 9b and c, respectively, for different values of the fractional order α. Observations similar to the previous ones hold also for the present case. Here we want just to emphasize that deviations from linearity in the strain fields are generated by the borders and by the sharp point of the stress field at the mid-span (see Fig. 9c). Note that all the strain curves intersect each other at the same point, as occurs in the stretched bar of Fig. 6c. Furthermore, and differently from the case of Fig. 8a, the geometry depicted in Fig. 9a is statically indeterminate, i.e. the stress field cannot be obtained simply by equilibrium equations or symmetry reasons. The resulting stress field is plotted in Fig. 9d. With respect to a local elastic material, for which the stress at the left edge is three times the value at the right extreme, the fractional model provides a more uniform solution (the ratio between the two reactions tending slowly towards two as $\alpha \to 0$).

We conclude this series of examples by remarking the basic difference with respect to the Eringen nonlocal model: the relative values of the displacement/strain solutions do not vary with the size but, because of the normalization factor, their absolute values are proportional to the size (i.e. the bar length) raised to a non-integer exponent. This is a peculiarity of the fractional model; coherently the size effect vanishes for $\alpha \to 1$, when l disappears from the normalization factor (see e.g. the strain in Fig. 8c).

6 Conclusions

In the present paper the mechanical behaviour of one-dimensional structures made of a material whose constitutive law provides the stress as the fractional integral of the strain field has been investigated. The nonlocality of fractional derivatives has thus been exploited to take long-range material interactions into account. Up to some extent, the present fractional nonlocal elastic model can be seen as a particular case of the more general Eringen nonlocal elasticity theory. However there are some differences that have been outlined in the paper and that make the model applicable to a distinct class of materials: the nonlocality of the fractional model seems to be stronger, affecting the overall mechanical behaviour and giving rise to non-standard, power law size effects. Furthermore, possible connections with gradient elasticity and peridynamic theory have been analyzed and recent results in the Scientific Literature dealing with fractional calculus and nonlocal elasticity have been briefly reviewed.

An original analytical result has been proved and exploited to show that the fractional nonlocal model is the continuum limit of a discrete lattice with three levels of long-range interactions described by springs whose stiffness decays with the power law of the distance between the connected points. This equivalence provides a new mechanical insight into the fractional model, showing that it is able to capture also the interactions between bulk and surface material points. The fractional differential problem ruling the mechanical behaviour of a one-dimensional fractional nonlocal elastic structure has been set, either with static or kinematic boundary conditions. A suitable numerical algorithm has been finally developed and applied to some example problems.

References

1. Mainardi F (2010) Fractional calculus and waves in linear viscoelasticity: an introduction to mathematical models. Imperial College Press, London
2. Rossikhin YA, Shitikova MV (2010) Application of fractional calculus for dynamic problems of solid mechanics: novel trends and recent results. Appl Mech Rev 63(010801):1–52
3. Mainardi F, Luchko Y, Pagnini G (2001) The fundamental solution of the space-time fractional diffusion equation. Fract Calc Appl Anal 4:153–192
4. Metzler R, Nonnenmacher TF (2002) Space- and time-fractional diffusion and wave equations, fractional Fokker–Planck equations, and physical motivation. Chem Phys 284:67–90
5. Zoia A, Rosso A, Kardar M (2007) Fractional laplacian in bounded domains. Phys Rev E 76(021116):1–11
6. Magin RL, Abdullah O, Baleanu D, Zhou XJ (2008) Anomalous diffusion expressed through fractional order differential operators in the Bloch–Torrey equation. J Magn Reson 190:255–270
7. Macdonald JR, Evangelista LR, Lenzi EK, Barbero G (2011) Comparison of impedance spectroscopy expressions and responses of alternate anomalous Poisson–Nernst–Planck diffusion equations for finite-length situations. J Phys Chem C 115:7648–7655
8. Carpinteri A, Cornetti P (2002) A fractional calculus approach to the description of stress and strain localization in fractal media. Chaos, Solitons Fractals 13:85–94
9. Carpinteri A, Chiaia B, Cornetti P (2001) Static-kinematic duality and the principle of virtual work in the mechanics of fractal media. Comput Meth Appl Mech Eng 191:3–19
10. Tarasov VE (2005) Continuous medium model for fractal media. Phys Lett A 336:167–174

11. Michelitsch TM, Maugin GA, Rahman M, Derogar S, Nowakowski AF, Nicolleau FCGA (2012) An approach to generalized one-dimensional self-similar elasticity. Int J Eng Sci 61:103–111
12. Carpinteri A, Cornetti P, Sapora A (2009) Static-kinematic fractional operators for fractal and non-local solids. ZAMM-Z Angew Math Mech 89:207–217
13. Lazopoulos KA (2006) Non-local continuum mechanics and fractional calculus. Mech Res Commun 33:753–757
14. Di Paola M, Zingales M (2008) Long-range cohesive interactions of nonlocal continuum mechanics faced by fractional calculus. Int J Solids Struct 45:5642–5659
15. Carpinteri A, Cornetti P, Sapora A, Di Paola M, Zingales M (2009) An explicit mechanical interpretation of Eringen non-local elasticity by means of fractional calculus. In: Proceedings of 19th Italian Conference on Theoretical and Applied Mechanics, Ancona, Italy, 14–17 September 2009
16. Carpinteri A, Cornetti P, Sapora A (2011) A fractional calculus approach to nonlocal elasticity. Eur Phys J 193:193–204
17. Atanackovič TM, Stankovič B (2009) Generalized wave equation in nonlocal elasticity. Acta Mech 208:1–10
18. Cottone G, Di Paola M, Zingales M (2009) Elastic waves propagation in 1D fractional non-local continuum. Phys E 42:95–103
19. Sapora A, Cornetti P, Carpinteri A (2013) Wave propagation in nonlocal elastic continua modelled by a fractional calculus approach. Commun Nonlinear Sci Numer Simul 18:63–74
20. Challamel N, Zorica D, Atanackovič TM, Spasič DT (2013) On the fractional generalization of Eringen's nonlocal elasticity for wave propagation. C R Mec 341:298–303
21. Drapaca CS, Sivaloganathan S (2012) A fractional model of continuum mechanics. J Elast 107:105–123
22. Tarasov VE (2006) Continuous limit of discrete systems with long-range interaction. J Phys A 39:14895–14910
23. Tarasov VE (2013) Lattice model with power-law spatial dispersion for fractional elasticity. Cent Eur J Phys 11:1580–1588
24. Oldham KB, Spanier J (1974) The fractional calculus. Academic Press, New York
25. Samko G, Kilbas AA, Marichev OI (1993) Fractional integrals and derivatives. Gordon and Breach, Amsterdam
26. Podlubny I (1999) Fractional differential equations. Academic Press, San Diego
27. Agrawal OP (2007) Fractional variational calculus in terms of Riesz fractional derivatives. J Phys A 40:6287–6303
28. Gorenflo R, Mainardi F (2001) Random walk models approximating symmetric space-fractional diffusion processes. In: Elschner J, Gohberg I, Silbermann B (eds) Problems in mathematical physics (Siegfried Prössdorf Memorial Volume). Birkhäuser Verlag, Boston-Basel-Berlin, pp 120–145
29. Mainardi F, Gorenflo R, Moretti D, Pagnini G, Paradisi P (2002) Discrete random walk models for space-time fractional diffusion. Chem Phys 284:521–541
30. Ortigueira MD (2008) Fractional central differences and derivatives. J Vib Control 14:1255–1266
31. Kröner E (1967) Elasticity theory of materials with long range cohesive forces. Int J Solids Struct 3:731–742
32. Eringen AC (1978) Line crack subjected to shear. Int J Fract 14:367–379
33. Polizzotto C (2001) Non local elasticity and related variational principles. Int J Solids Struct 38:7359–7380
34. Silling SA (2000) Reformulation of elasticity theory for discontinuities and long-range forces. J Mech Phys Solids 48:175–209
35. Silling SA, Zimmermann M, Abeyaratne R (2003) Deformation of a peridynamic bar. J Elast 73:173–190
36. Aifantis EC (1999) Gradient deformation models at nano, micro, and macro scales. J Eng Mater 121:189–202
37. Metrikine AV, Askes H (2002) One-dimensional dynamically consistent gradient elasticity models derived from a discrete microstructure. Part 1: generic formulation. Eur J Mech A 21:555–572
38. Sumelka W, Blaszczyk T (2014) Fractional continua for linear elasticity. Arch Mech 66:147–172
39. Carpinteri A, Mainardi F (1997) Fractals and fractional calculus in continuum mechanics. Springer-Verlag, Wien
40. Yang Q, Liu F, Turner I (2010) Numerical methods for fractional partial differential equations with Riesz space fractional derivatives. Appl Math Model 34:200–218